Hindawi
International Journal of Antennas and Propagation
Volume 2022, Article ID 1801213, 6 pages
https://doi.org/10.1155/2022/1801213

Research Article

A Wideband Antenna for GNSS Applications with Improved Orthogonal Dipole

Lin Daming,[1] Wang Encheng ,[2] and Wang Jie[3]

[1]*Research Institute of Highway, Ministry of Transport, Beijing 100088, China*
[2]*Information Engineering College of North China University of Technology, Beijing 100044, China*
[3]*College of Civil Engineering of North China University of Technology, Beijing 100044, China*

Correspondence should be addressed to Wang Encheng; dlenchw@hotmail.com

Received 6 July 2022; Revised 11 September 2022; Accepted 20 September 2022; Published 11 October 2022

Academic Editor: Trushit Upadhyaya

This letter presents a wideband antenna for high-precision Global Navigation Satellite System (GNSS) applications. The antenna consists of a pair of improved orthogonal dipoles that are fed by a feed network with Composite Right/Left-Handed Transmission Lines (CRLH-TLs), a polygonal patch, and a reflector. By using improved orthogonal dipole, the beamwidth of the antenna is broadened. The CRLH-TLs is adopted in feed network to obtain outputs with stable phase difference. Experiment results indicate that the antenna has a less than 10-dB return-loss bandwidth in the range of 1.1 to 1.7 GHz, a 3-dB axial-ratio bandwidth from 1.2 to 1.6 GHz, and a larger than 6.37 dBi gain in the whole operating band. The measured results show that the proposed antenna has stable performance in the whole operating band, which means that it is a suitable antenna used for GNSS applications.

1. Introduction

The global navigation satellite systems, such as Global Positioning System (GPS), GLONASS, Galileo, and BDS, have been used in many areas such as navigation, positioning, geographic surveys, time standards, and meteorology. Accuracies on the order of centimeters and millimeters are required in many high precision applications [1, 2]. However, multipath error continues to be a major limiting factor in realizing the level of accuracy [3–5]. To maintain high accuracy in GNSS, the multipath signals received by the system, which are created by reflections from nearby obstacles, should be mitigated. To provide high possible position accuracy in multipath environments, GNSS antennas shall be designed to radiate in right-hand circular polarization (RHCP) and suppress left-hand circular polarized (LHCP) modes to be resilient against multipath errors. Therefore, GNSS antennas must have high gain, good axial ratio bandwidth, and stable phase center [6].

The bandwidth of the conventional microstrip antenna design is narrow [7]. Many new antenna and GNSS antenna designs have been proposed for dual- or multiband operation [8–12]. In Reference [8], a low-profile, tri-band, wide slot antenna for the wireless local area network (WLAN) and world-wide interoperability for microwave access (WiMAX) applications is proposed. In Reference [9], a hexaband, quad-circular-polarization (CP) slotted patch antenna for 5G, GPS, LTE, and radio navigation applications is proposed. A compact dual-band circularly polarized microstrip ring antenna for GPS $L1$ and $L2$ bands is proposed in Reference [10]. In Reference [11], an improved feed network with $\pm 8^{\circ}$ phase imbalance is designed to be used in the CP antenna. A compact CP multimode antenna for global navigation satellite system reflectometry is presented in Reference [12]. In Reference [13], a microstrip feed two pentagon-shaped dielectric resonator antenna array network is presented. Concept of a defected ground has been integrated to improve impedance bandwidth. In Reference [14], a 1×4 cylindrical dielectric resonator antenna (CDRA) array is successfully developed and presented. The claimed structure has introduced quarter wavelength transformer with power divider network. The adopted concept gives adequate response in terms of appropriate suppression, phase distribution, and power division.

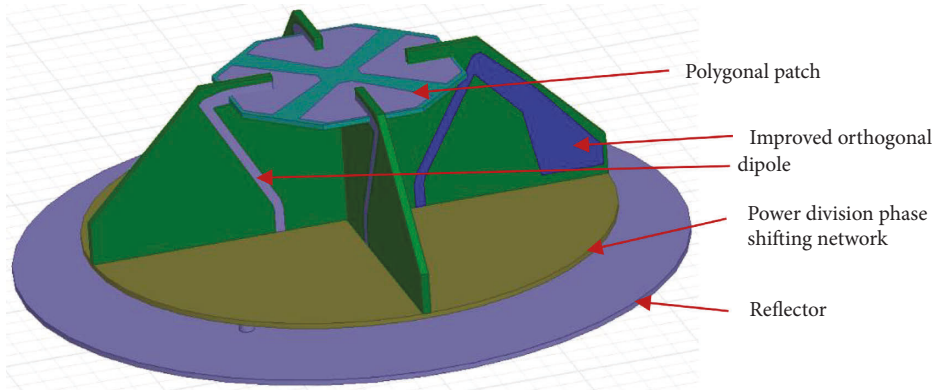

Figure 1: Geometry of the proposed antenna.

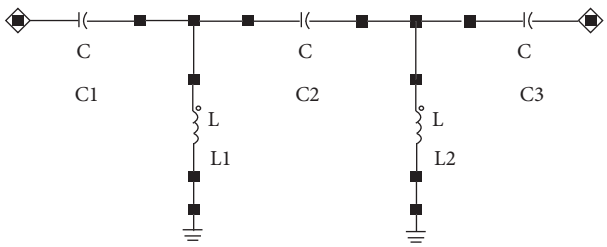

Figure 2: Equivalent circuit of CRLH-TLS structure.

In this paper, a new wideband CP antenna for GNSS is presented. The proposed antenna consists of a pair of improved orthogonal dipoles, a polygonal patch, and a reflector. The improved orthogonal dipoles help the antenna to obtain better symmetrical radiation pattern. A polygonal patch is used to achieve better antenna gain. In addition, a power division phase shifting network with less phase difference fluctuation is developed, which can help the antenna to obtain better axial ratio bandwidth. The proposed antenna is simulated using the HFSS and validated by measurement.

2. Antenna Design

2.1. Antenna Geometry. The geometry of the proposed antenna is shown in Figure 1. The design idea of the antenna is that two linearly polarized antennas are fed by a power division phase shifting network, so that the two linearly polarized antennas generate two orthogonal modes with a 90 phase difference and therefore causes a CP radiation. The reflector is fabricated from an aluminum plate with a thickness of 1 mm, and other parts are printed on the FR4 substrate with a relative permittivity of 4.32, loss tangent of 0.0027, and a thickness of 2 mm. Detailed parametric study of this antenna is listed in the following section.

2.2. Design of Power Division Phase Shifting Network. Power division phase shifting network is the basic and important component in GNSS antenna. A broadband feed network with CRLH-TLS is used to obtain the required phase shift and improve the axial ratio in the direction of maximum radiation, as shown in Figure 2.

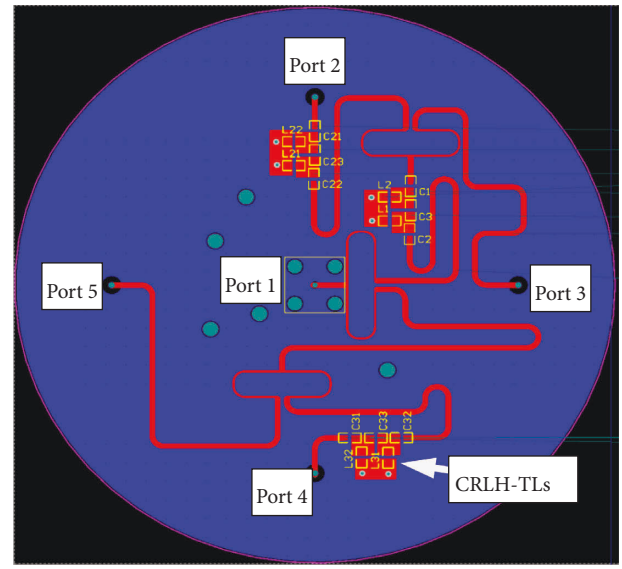

Figure 3: PCB structure of the power division phase shifting network.

Figure 3 shows the printed circuit board (PCB) structure of the power division phase shifting network, Port1 is the input port, and other ports are output ports. The power division phase shifting network can provide four ways of equal magnitude signals with stable phase differences of 0°, 90°, 180°, and 270° in the whole band.

Figure 4 shows the simulation result of $S21$, $S31$, $S41$, and $S51$ when using CRLH-TLS. A stable phase difference between the output ports can be obtained by optimizing the capacitance and inductance values. The values of $L1$ and $L2$ are 12 nH, $C1$ and $C3$ are 5.1 pF, and $C2$ are 9.1 pF.

2.3. Parametric Study of the Designed Antenna. As we know, an electric dipole has an 8-shaped radiation pattern on the E-plane and an O-shaped pattern on the H-plane, and the radiation pattern of a magnetic dipole is opposite to that. As the basic unit, the linear polarization antenna adopts a microstrip-fed dipole antenna. The dipole length of an ideal symmetric dipole antenna is 0.5λ. In order to increase the working bandwidth of the antenna, we shorten the length of

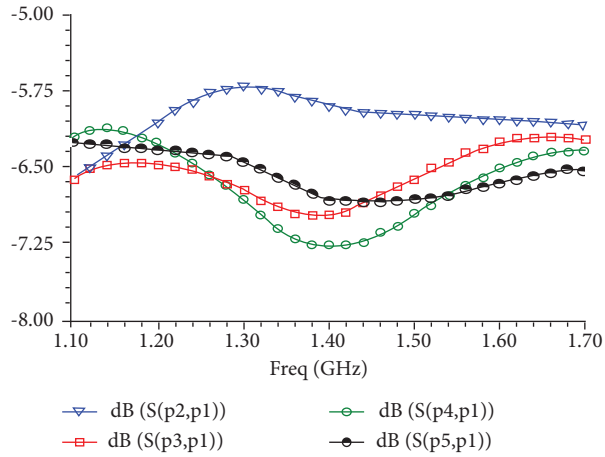

Figure 4: Simulation result of *S*21, *S*31, *S*41, and *S*51.

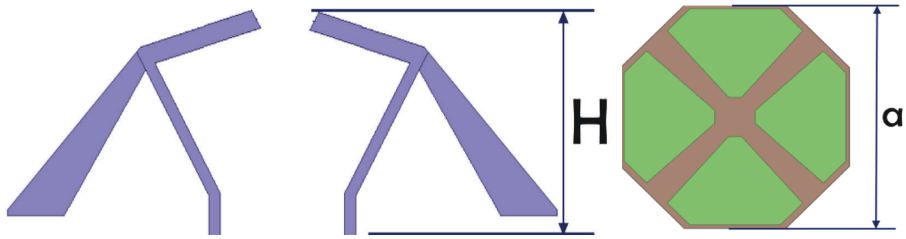

Figure 5: Structure of the improved dipole and the patch.

the dipole by widening the width of the dipole. By taking such measures, both the impedance and the gain bandwidth of the antenna can be increased. Of course, this will slightly reduce the antenna gain.

According to the requirements of high-precision GNSS applications, the 3 dB beamwidth of the antenna radiation pattern is needed to exceed 100°, which is difficult to achieve by a single dipole antenna. This problem can be solved by placing two antennas of the same polarization symmetrically on the reflector. At the same time, the dipole arms are tilted downward to present a semicircular shape, which can broaden the beamwidth of the radiation pattern.

In order to obtain better beam width and compact structure of the antenna, we shorten the length of adjacent dipoles and deform dipoles into polygonal patch, so as to ensure that the resonant frequency of the antenna is within the working frequency band.

The structure of the improved dipole and the patch is shown in Figure 5.

The influence of the height of the dipole antenna and the size of the patch on the *S*11 of the antenna is simulated, and the results are as shown in Figures 6 and 7.

As shown in Figure 6, in the low-frequency band, the impedance bandwidth of the antenna becomes wider with the increase of the dipole height; in the high-frequency band, the *S*11 value at the resonance point decreases with the increase of the dipole height. A similar conclusion can also be seen from Figure 7. Figure 8 shows the optimized dimensions of the dipole and the patch.

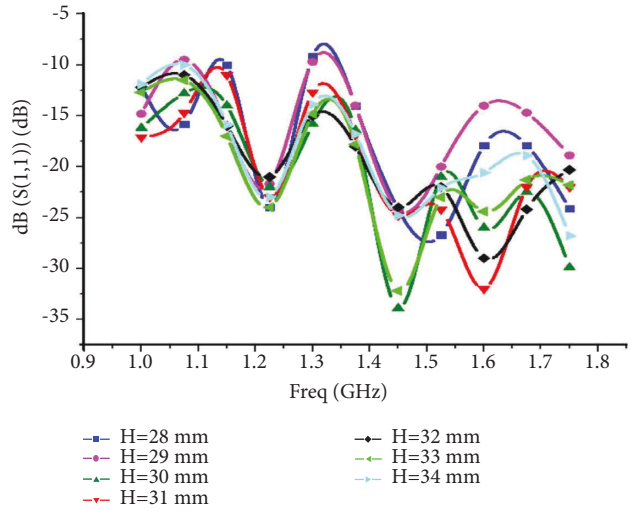

Figure 6: S_{11} at various dipole heights.

The reflector and PCB can weaken the backward radiation of the antenna through secondary reflection. The electromagnetic waves radiating back will oscillate repeatedly between the reflector and the PCB and eventually disappear. The radius of the reflector depends on the effective electrical length of its corresponding dipole, which is approximately 0.45λ (101 mm) and 0.59λ (130 mm). The distance between the reflector and the PCB is approximately $0.022\ \lambda$ (5 mm). The overall size of the antenna is $130\text{ mm} * 130\text{ mm} * 39\text{ mm}\ 0.48 \times 0.48 \times 0.14\lambda_0^3$($\lambda_0$ is the wavelength in the air at 1.1 GHz).

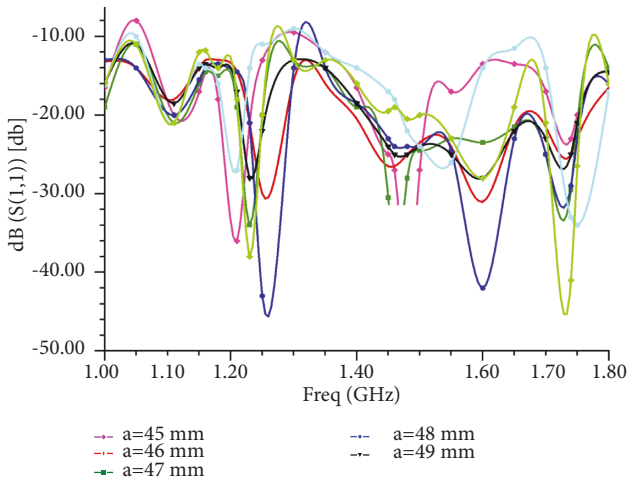

Figure 7: S_{11} at various patch sizes.

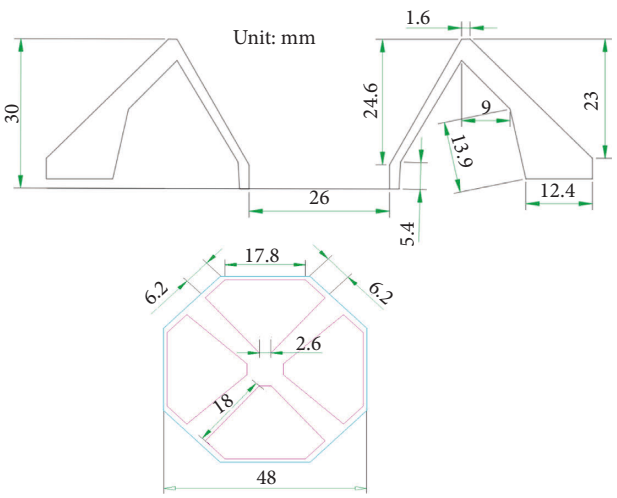

Figure 8: Detailed dimensions of the dipole and patch (unit: mm).

3. Results and Discussion

The designed antenna is fabricated, as shown in Figure 9. This antenna was also tested, and the results are shown in Figures 10–12. Figure 10 shows the measured radiation pattern at 1227 MHz, Figure 11 shows the simulated and measured gain of the antenna in the entire frequency band, while Figure 12 shows the simulated and measured S11 and axial ratio of the antenna.

At the same time, the performance of this antenna with other similar antennas was compared, and the results are as shown in Table 1.

From Table 1, it can be seen that the impedance bandwidth of the antenna is 43%, and the measured gains in the band are higher than 6 dBi. The 3 dB axial ratio bandwidth of the antenna is about 30%, which can be used in high-precision navigation systems. The antenna achieves better performance at a lower cost.

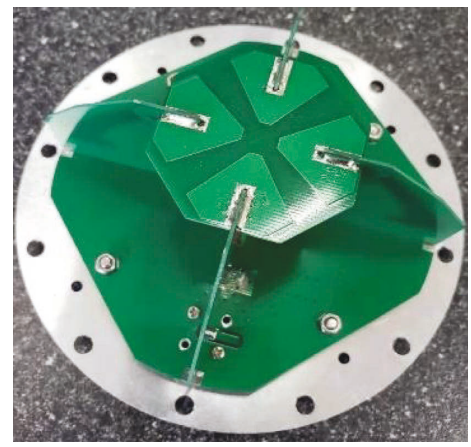

Figure 9: Fabricated antenna.

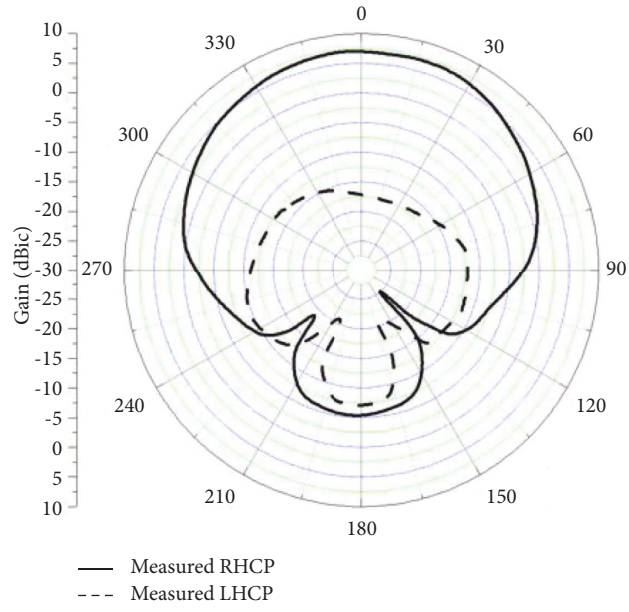

Figure 10: Measured radiation pattern at 1227 MHz.

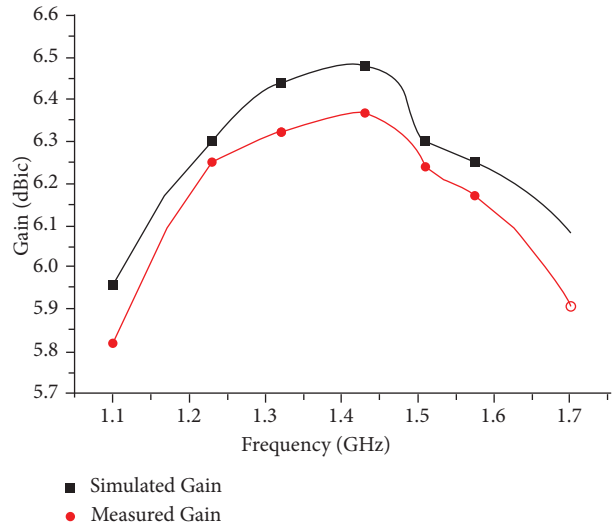

Figure 11: Simulated and measured gain of the antenna.

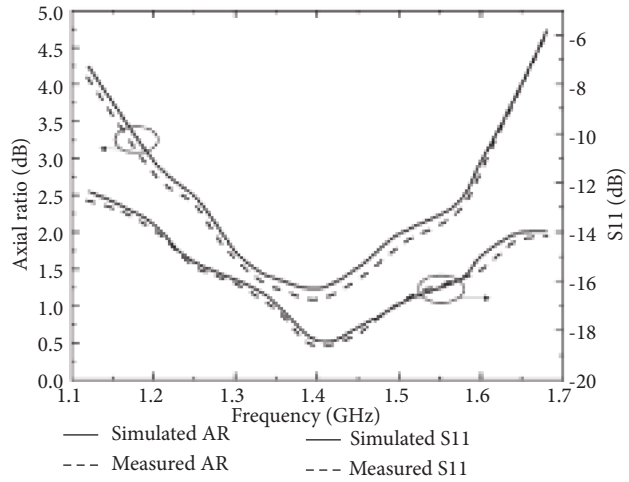

Figure 12: Simulated and measured AR and *S*11 of the antenna.

Table 1: Comparison of the proposed antenna with similar antennas.

Reference	Dimension (λ_0※)	ARBW (GHz)	IPBW (GHz)	Gain (dBic)	Substrate material
[15]	$0.3 \times 0.64 \times 0.64\lambda_0^3$@1.16 GHz	1.22 to 1.6	1.16 to 1.61	6	RT/duroid 5880
[16]	$0.38 \times 0.38 \times 0.07\lambda_0^3$@1.518 GHz	1.5 to 1.67	1.479 to 1.683	5.2	RO4003
[17]	$0.37 \times 0.42 \times 0.03\lambda_0^3$@1.575 GHz	1.57 to 1.605	1.565 to 1.655	4.65	RO4003C
[18]	$0.7 \times 0.8 \times 0.09\lambda_0^3$@1.8 GHz	0.93 to 2.71	1.13 to 2.51	5	RO4350B
[19]	$0.2 \times 0.2 \times 0.05\lambda_0^3$@1.2 GHz	1.1 to 1.6	1.1 to 1.6	7	Rogers TMM6
Proposed	$0.48 \times 0.48 \times 0.14\lambda_0^3$@1.1 GHz	1.1 to 1.6	1.2 to 1.7	6.37	FR4

※λ_0 is the wavelength in the air at the specific frequency.

4. Conclusion

In this paper, a wideband antenna for GNSS applications is proposed. In order to improve the multipath mitigation performance, the proposed antenna is fed by a new power division phase shifting network with CRLH-TLS. The bandwidth and gain of the antenna are increased by improving the conventional electromagnetic dipole antenna. Circularly polarized radiation with wide 3 dB-AR beamwidth covers the whole GNSS bands. Simulated and measured results indicate that the proposed antenna is applicable for GNSS with high precision.

Data Availability

The test result data used to support the findings of this study are included within the article.

Conflicts of Interest

The authors declare that they have no conflicts of interest.

Acknowledgments

This work is partially supported by the Research on Key Technologies for Accurate Positioning of BINGTUAN Transportation Key Vehicles and Infrastructure based on Beidou (Grant No.: 2108AB028) and the Project of Young Yuyou of North China University of Technology, 2018.

References

[1] S. Liu, D. Li, B. Li, and F. Wang, "A compact high-precision GNSS antenna with a miniaturized choke ring," *IEEE Antennas and Wireless Propagation Letters*, vol. 16, pp. 2465–2468, 2017.

[2] E. R. Gafarov, A. A. Erokhin, and Y. P. Salomatov, "The GNSS helix antenna for high precision application," in *Proceedings of the 2019 Radiation and Scattering of Electromagnetic Waves (RSEMW)*, pp. 128–131, Divnomorskoe, Russia, June 2019.

[3] A. Boccia, Di Massa, and Di Massa, "A dual frequency microstrip patch antenna for high-precision GPS applications," *IEEE Antennas and Wireless Propagation Letters*, vol. 3, pp. 157–160, 2004.

[4] C. C. Counselman, "Multipath-rejecting GPS antennas," *Proceedings of the IEEE*, vol. 87, no. 1, pp. 86–91, 1999.

[5] W. EnCheng, W. Zhuopeng, and C. Zhang, "A wideband Antenna for global navigation satellite system with reduced multipath effect," *IEEE Antennas and Wireless Propagation Letters*, vol. 12, pp. 124–127, 2013.

[6] M. K. Emara, J. Hautcoeur, G. Panther, J. S. Wight, and S. Gupta, "Surface impedance engineered low-profile dual-band grooved-dielectric choke ring for GNSS applications," *IEEE Transactions on Antennas and Propagation*, vol. 67, no. 3, pp. 2008–2011, 2019.

[7] S. Lee, Y. Yang, K.-Y. Lee, and K. C. Hwang, "Dual-band circularly polarized annular slot antenna with a lumped inductor for GPS application," *IEEE Transactions on Antennas and Propagation*, vol. 68, no. 12, pp. 8197–8202, 2020.

[8] U. Patel, M. Parekh, and A. Desai, "Wide slot tri band antenna for wireless local area network/worldwide interoperability for

Microwave access applications," *International Journal of Communication Systems*, vol. 7, 2021.

[9] A. Abdalrazik, A. Gomaa, and A. A. Kishk, "A hexaband quad-circular-polarization slotted patch antenna for 5G, GPS, WLAN, LTE, and radio navigation applications," *IEEE Antennas and Wireless Propagation Letters*, vol. 20, no. 8, pp. 1438–1442, 2021.

[10] J. Yuan, Z. Chen, Z. D. Chen, and Y. Li, "A compact dual-band microstrip ring antenna using multiring ground for GPS L1/L2-band," *IEEE Antennas and Wireless Propagation Letters*, vol. 20, no. 12, pp. 2250–2254, 2021.

[11] F. Tamjid, F. Foroughian, C. M. Thomas, A. Ghahreamani, R. Kazemi, and A. E. Fathy, "Toward high-performance wideband GNSS antennas-design tradeoffs and development of wideband feed network structure," *IEEE Transactions on Antennas and Propagation*, vol. 68, no. 8, pp. 5796–5806, 2020.

[12] A. M. Musthafa, M. Khalily, A. Araghi, O. Yurduseven, and R. Tafazolli, "Compact multimode quadrifilar helical antenna for GNSS-R applications," *IEEE Antennas and Wireless Propagation Letters*, vol. 21, no. 4, pp. 755–759, April 2022.

[13] A. Vahora and K. Pandya, "Microstrip feed two elements pentagon dielectric resonator antenna array," in *Proceedings of the 2019 International Conference on Innovative Trends and Advances in Engineering and Technology (ICITAET)*, pp. 22–25, Shegoaon, India, December 2019.

[14] A. Vahora and K. Pandya, "Triple band dielectric resonator antenna array using power divider network technique for GPS navigation/bluetooth/satellite applications," *International Journal of Microwave and Optical Technology*, vol. 15, no. 4, pp. 369–378, 2020.

[15] D.-C. Chang and H.-J. Lee, "A wideband circularly polarized antenna for GNSS," in *Proceedings of the 2016 IEEE 5th Asia-Pacific Conference on Antennas and Propagation (APCAP)*, pp. 343-344, Kaohsiung, Taiwan, July 2016.

[16] E. R. Gafarov, A. V. Stankovsky, and Y. P. Salomatov, "A GNSS dipole antenna with a meander-line polarizer for the reduction of multipath interference," in *Proceedings of the 2017 Radiation and Scattering of Electromagnetic Waves (RSEMW)*, pp. 311–313, Divnomorskoe, Russia, June 2017.

[17] X. Q. Nasimuddin, X. Qing, and Z. N. Chen, "A compact circularly polarized slotted patch antenna for GNSS applications," *IEEE Transactions on Antennas and Propagation*, vol. 62, no. 12, pp. 6506–6509, 2014.

[18] L. Qiang, L. Yong, and Z. Mo, "Compact broadband circularly-polarized directional universal GNSS antenna with symmetric radiation pattern and stable near-zenith coverage," *IET Microwaves, Antennas & Propagation*, vol. 11, no. 5, pp. 657–663, 2016.

[19] C. Sun, Z. Wu, and B. Bai, "A novel compact wideband patch antenna for GNSS application," *IEEE Transactions on Antennas and Propagation*, vol. 65, no. 12, pp. 7334–7339, 2017.